

Online Research @ Cardiff

This is an Open Access document downloaded from ORCA, Cardiff University's institutional repository: <https://orca.cardiff.ac.uk/id/eprint/73836/>

This is the author's version of a work that was submitted to / accepted for publication.

Citation for final published version:

Perisoglou, Emmanouil and Dixon, Dylan 2015. Experimental monitoring of different dimensions of transpired solar collectors. *Energy Procedia* 70 , pp. 111-120. 10.1016/j.egypro.2015.02.105 file

Publishers page: <http://dx.doi.org/10.1016/j.egypro.2015.02.105>
<<http://dx.doi.org/10.1016/j.egypro.2015.02.105>>

Please note:

Changes made as a result of publishing processes such as copy-editing, formatting and page numbers may not be reflected in this version. For the definitive version of this publication, please refer to the published source. You are advised to consult the publisher's version if you wish to cite this paper.

This version is being made available in accordance with publisher policies.

See

<http://orca.cf.ac.uk/policies.html> for usage policies. Copyright and moral rights for publications made available in ORCA are retained by the copyright holders.



International Conference on Solar Heating and Cooling for Buildings and Industry, SHC 2014

Experimental monitoring of different dimensions of transpired solar collectors

Emmanouil Perisoglou^a, Dylan Dixon^a

^aWelsh School of Architecture, Cardiff University, Bute Building, King Edward VII Avenue, Cardiff CF10 3NB, UK

Abstract

This study analyses the parameters concerning the performance of Transpired Solar Collectors (TSCs) and offers a monitoring methodology that addresses some of the potential errors and uncertainties, including instrumentation use. The study also investigates three TSC modules of equal area but different dimensions and compares their efficiencies by altering several parameters. The cavity of the systems is also monitored for different fan velocities and for different wind directions. The experiments took place outdoors in order to simulate real life installations.

© 2015 The Authors. Published by Elsevier Ltd. This is an open access article under the CC BY-NC-ND license (<http://creativecommons.org/licenses/by-nc-nd/4.0/>).

Peer-review by the scientific conference committee of SHC 2014 under responsibility of PSE AG

Keywords: Transpired; Solar; Collector; Monitoring; Efficiency; Performance; Measurement; Instrumentation

1. Introduction

A Transpired Solar Collector (TSC) is a solar thermal technology which heats or preheats the ventilation air supply to buildings and can be intergraded into the building envelope [1]. The Sustainable Building Envelope Demonstration (SBED) project aims to accelerate the development of innovative TSC technology through demonstrating installations on eight buildings in-use[2]. In order to create a robust monitoring methodology the project tested a number of monitoring techniques in three experimental TSC modules on the roof of the Welsh School of Architecture (WSA), Cardiff University. Part of the collected data was analysed and the performance of the TSCs was evaluated and is included in this study. Additionally, this study suggests practical guidelines regarding instrumentation and analysis, in order to get accurate and reliable results.

Nomenclature

A_p	projected area of the TSC(m ²)
A_d	duct cross sectional area
C_p	specific heat of air (1.007 to 1.048 kJ/kg.K around environmental conditions at 1 atm pressure [3, 4])
I	solar radiation (W/m ²)
\dot{m}	air mass flow rate (kg/s)
T_{amb}	ambient air temperature (K or °C)
T_{out}	air temperature at the TSC outlet (K or °C)
T_{rise}	air temperature rise caused by the TSC (K or °C)
Q	TSC heat delivery (W)
u_d	centreline duct air velocity (m/s)
u_a	average duct air velocity
β	duct velocity coefficient =0.86 [5]
η	instantaneous efficiency of the collector
ρ	average density of air in the collector (kg/m ³)

2. TSCs efficiency

Kutscher et al was the first who examined the technology and introduced the basic instantaneous efficiency equation (1), which is widely used as the basic indicator of TSC performance [6-8].

$$\eta = \frac{\dot{m} C_p T_{rise}}{I A_p} \quad (1)$$

$$\text{where } T_{rise} = T_{out} - T_{amb} \quad \text{and} \quad Q = \dot{m} C_p T_{rise} \quad (2)$$

Air mass flow rate in a duct could be calculated by measuring the velocity in the pipe for a known diameter (equation 3).

$$\dot{m} = \rho \beta u_d A_d \quad (3)$$

By using modeling and laboratory experiments the technology has been studied and optimized to a certain extent. On the other hand, there is a lack of data regarding real installations as few have been monitored. Additionally, most of the existing performance data of TSC installations refer to those in North America where the climate is different to Europe and direct performance comparisons are potentially misleading [1].

Monitoring approaches vary considerably between investigations and there is little guidance regarding instrumentation quality and positioning, both of which can have a significant impact on the confidence of results.

3. Experimental methodology

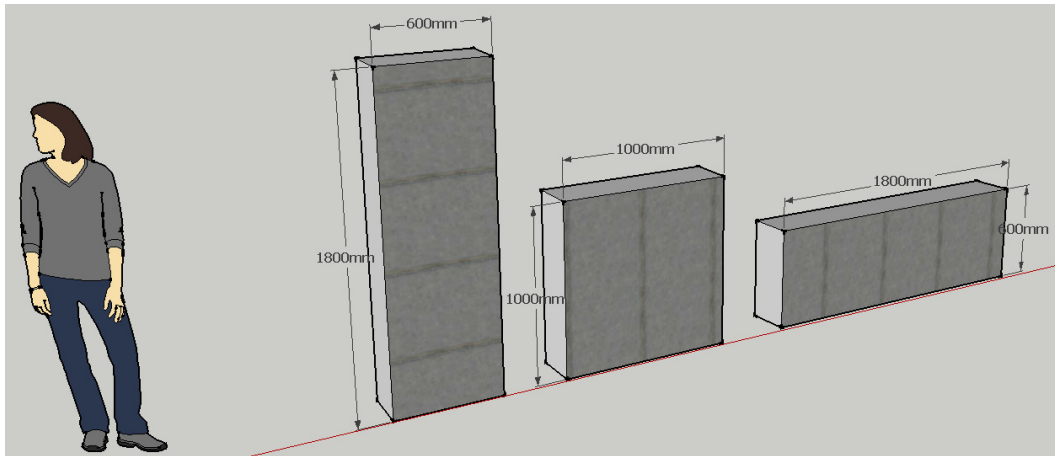


Fig. 1. Vertical (A), Square (B) and Horizontal (C) TSC Test Rig on the Roof of the Institute

A vertical (A), a square (B) and a horizontal (C) experimental module were placed vertically on the WSA's flat roof. All three collectors (Fig 1) having the same absorbing area (1m^2) similar to experimental studies [9-12]. Three variable speed fans were placed behind the TSCs in order to draw air through a ducting system, while the orientation, materials, perforation pattern, hole diameter, insulation, back wall, cavity width, as well as extraction position and diameter were exactly the same in order to facilitate comparisons. Data were collected for all the TSCs together using synchronized high quality data loggers. A meteorological station was also placed to capture wind speed, wind direction and rain data. Measurements were collected for different flows under stable solar radiation conditions (clear sky) and during windy and non-windy days. Furthermore, the mass flow rate and the pressure inside the cavity was kept similar for the three collectors for each set of measurements. The equations used for heat delivery and efficiency were based on the most commonly used methodology for the evaluation of TSC performance [13]. Statistical analysis was used to minimise data errors and estimate uncertainties.

4. Instrumentation

The instantaneous efficiency equation (1), which is a fundamental indicator of the TSCs performance, has 5 different components. A close view of the equations elements and a robust metrological approach improves the confidence level of the results. For this reason a breakdown of the efficiency puzzle follows below.

4.1. Mass flow rate (\dot{m})

The mass flow rate was calculated from measurements of air velocity in the system duct using the mass flow formula in equation (4); the β correction factor was not included to normalise the velocity as each duct flow was subject to a validation process described below.

$$\dot{m} = \rho u_a A_d \quad (4)$$

With a possible temperature range of 50°C or more, the density of air within a TSC could vary more than 15%. As such, values for air density, at 2°C intervals, were taken from reference CIBSE tables [4]. Humidity and atmospheric pressure influences on density were ignored with estimated uncertainties in the region of $<1\%$ and $\pm 1.2\%$ respectively. The location of the test site was considered to be at sea level and standard atmospheric pressure 101 325 Pa was used.

A 0.1m diameter duct was used to extract air from each TSC and thought to be in reasonable proportion to the 1m² surface area of the TSC. The internal diameter of the ducting was measured at 0.097m, giving a cross-sectional area of 0.0074m².

A minimum duct velocity of 1.5m/s was chosen to create a 25 Pa pressure drop in the holes which is the minimum pressure drop in order to avoid flow reversals in the cavity. With a cross-sectional area and minimum duct velocity, the condition in the duct were predicted to be turbulent (Reynolds number $\approx 10\,500$).

Manufactures' advise against using differential pressure sensors in turbulent flow, so these were avoided initially. The size of the ducting also dictated the need for a small velocity sensor to minimise the disturbance to the air flow. As such, a small hotwire anemometer was used to take single point measurements at 0.24 x diameter (manufactures instructions). Despite the predicted turbulence, sensors were located more than 10 duct diameters from obstructions.

To counter the unreliable nature of single point airflow measurements a validation process, based on the Log Chebyshev method for circular ducting was used to improve reliability [14]; a second hotwire anemometer and a secondary data logger were used to take simultaneous readings every second for 60 seconds, at six different depths in 3 different projections across a section of the duct. The mean velocity from the second anemometer was then compared to the single point measurement and a correction factor was applied to the single point measurement, although agreement between the single point and multi-point averages was in the region of 95%.

4.2. Specific heat capacity (C_p)

The specific heat capacity of air is influenced by moisture content and temperature. Using standard equations from the ideal gas law, estimates for specific heat capacity were made utilising relative humidity and temperature data. Calculations suggested that the range of variation under typical TSC temperature and humidity for the UK might be between 1.007 to 1.048 kJ/kg.K, which agree with CIBSE published data [4].

4.3. Temperature rise ($Trise$)

The two fundamental temperatures considered were ambient air temperature (T_{amb}) and TSC output temperature (T_{out}). High quality thermometers were needed in both cases and for this reason the Pt100 Class A was selected. This choice was based on the accuracy of this type in comparison to thermistors and thermocouples as it performs better in environmental conditions and reasonably priced [15, 16]. The class A tolerance is specified in DIN/IEC751 as $\pm(0.15 + 0.002 \cdot t)^\circ\text{C}$ [17], which means that the sensors have a maximum inherent uncertainty range of $\pm 0.25^\circ\text{C}$ for the temperature range of this study. Pt100s also have a very good long term stability, linearity and excellent repeatability [15, 18]. However, Pt100 sensors are relatively thick, which could cause time response issues and flow obstruction. The 4 wire Pt100 was used in order to eliminate any wiring and connector error [19]. Also, all Pt100s used in the experiment were calibrated prior to use at 0°C , 20°C and 40°C by using a 4 wire Pt100 1/10DIN standard (± 0.15 uncertainty), an ice point Dewar and a stirring water bath device [20].

By its nature, a temperature sensor only measures the temperature of a specific point (assumption of minimum sensor dimensions). If only one sensor is available, careful consideration must be given to the selection of the most representative point prior to installation. As Pt100s absorb radiant heat, in the case of ambient air temperature measurement, the sensor has to be protected by using a radiation shield to avoid direct sunlight.

The ideal position for measuring ambient temperature would be on the south (or solar) face of the TSC, as this is where the TSC draws air from; air in that area may be subject to warming from other sources which could be considered legitimate influences such as the ground. A south facing location would require the exclusion of solar influence. While radiation shields provide a good degree of protection it is not uncommon for solar heating to elevate such readings. Locating the shield in a shaded area can reduce or exclude solar influence, however, if this shaded area is some distance away from the TSC intake, there is an unknown degree of error in the temperature data. If the shield is shaded from direct solar radiation it is also possible for the thermal mass of the shield to suppress temperature readings, particularly if it is a compact and poorly ventilated unit. Ideally, the ambient temperature sensor should be placed near the face of the TSC, although not shading it; housed in a light weight, well ventilated enclosure (perhaps aspirated) and protected from direct solar radiation by an independent shield and separate from the sensor housing.

The TSC output temperature was measured just after the collector's cavity at the beginning of the duct. The sensor was placed centrally in the duct, positioned to ensure contact with the duct was avoided and the insertion point carefully sealed.

4.4. Solar irradiation (I)

The aim was to measure the solar power that reached the panel which is caused by both direct and diffuse solar radiation. This can be calculated using a horizontal solar global radiation sensor but the diffuse radiation reaching the vertical panel will not be ideally replicated, for this reason solar radiation can be measured more accurately when the sensor duplicates the inclination of the collector [21]. The most commonly used instrument for global solar radiation is the pyranometer, which is a broadband instrument that measures global solar irradiance incoming from a 2π solid angle on a planar surface [22]. Accuracy improves when the pyranometer is installed very close to the collector, thereby receiving a similar amount of radiation, experiencing the same shading effects and similar solar reflections. As the pyranometer measurement is the only variable of the efficiency equation's denominator, accuracy is dominant for high efficiencies and a high quality instrument is necessary. Another important factor is the response time, as there is a measuring inertia for most commercial pyranometers. Especially when the sky is partly cloudy, it is possible for readings from one interval to be effected by the previous conditions, resulting in significant error.

4.5. Collector surface area (A_p)

Each TSC was designed to have an equal area, similar to that of other test rigs in previous publications [9-12]. The vertical and horizontal TSC consisted of two panels of 1800mm x 300mm, giving a surface area of 1.08m². The square TSC consisted of three panels of 1000mm x 350mm, a surface area of 1.05 m². The internal cavity was 220mm.

4.6. Supplementary instrumentation

Further instrumentation was used to help understand the behavior of the system and the distribution of heat across the cavity. This is not part of the efficiency equation but was included in this study as a means to understanding the thermal behavior of the air inside the cavities of the different shaped collectors. The topology of thermal variation in the collector could indicate reasons for any efficiency differences. From a metrological perspective, the temperature mapping of the cavity resembles the calibration of the isothermal or climatic chambers (NF-X15-140 and EURAMET cg-11 standards [23]). The cavities were fitted with an array of thermocouples separated by equal distance to create a homogeneous grid. Extra sensors could be added to measure the temperature variation of the cavity's depth. 24 thermocouples were installed in cavities A and C, and 12 in B. There are four reasons that thermocouples were selected instead of Pt100s for this set of measurements:

- Thermocouples are very small and they do not affect the air flow.
- More than 60 thermocouples were needed which cost 10 times less than the Pt100s.
- The temperature variation in the cavity is an instantaneous temperature snapshot; thus, time response is crucial and the thermocouples are very fast[15, 18].
- High accuracy of the "true value" is not a priority. The aim was to analyse the temperature variation within cavity.

Type T thermocouples were selected as they are the most accurate with a sensor uncertainty of $\pm 0.5^\circ\text{C}$ (ITS-90). Additionally, the range of type T matches the environmental range under investigation and has a very fast response [24]. Finally, to avoid long wiring extension of the thermocouples a multiplexer (data logger expansion unit) with an embodied reference temperature (cold junction [20]) was used.

5. Results and discussion

The graph below (figure 2) shows the efficiency of the three different collectors (A,B,C) for different flows. The measurements were captured for velocities from 1.5m/s to 5.5m/s ($42\text{m}^3/\text{h}$ to $155\text{ m}^3/\text{h}$ volume flow rate) for a 0.1m diameter pipe.

It seems that when the flow exceeds $120\text{m}^3/\text{h}$ the efficiency reaches a plateau. The horizontal collector seems to perform slightly better, reaching an efficiency close to 70% for the maximum flow. The temperature rise, as expected, falls with the higher flow and, again, the horizontal seems to deliver air at a marginally higher temperature.

The outlet for all the vertical collectors was positioned central to the cavity and approximately 100mm from the top edge. Undoubtedly, this position and the different shapes of the TSCs created different air flow behaviours and affected the suction distribution in the cavity. This is thought to be particularly relevant when comparing collectors A and C (vertical and horizontal), which present the greatest differences in dimensions. In the following graph (figure 3) the outlet temperature and the average cavity temperatures are presented for these two collectors. It seems that in low flows, the fans draw slightly colder air than the average cavity temperature, but at high flows the suction seems to work better, especially for the horizontal where the average cavity temperature is equal to the pipe temperature.

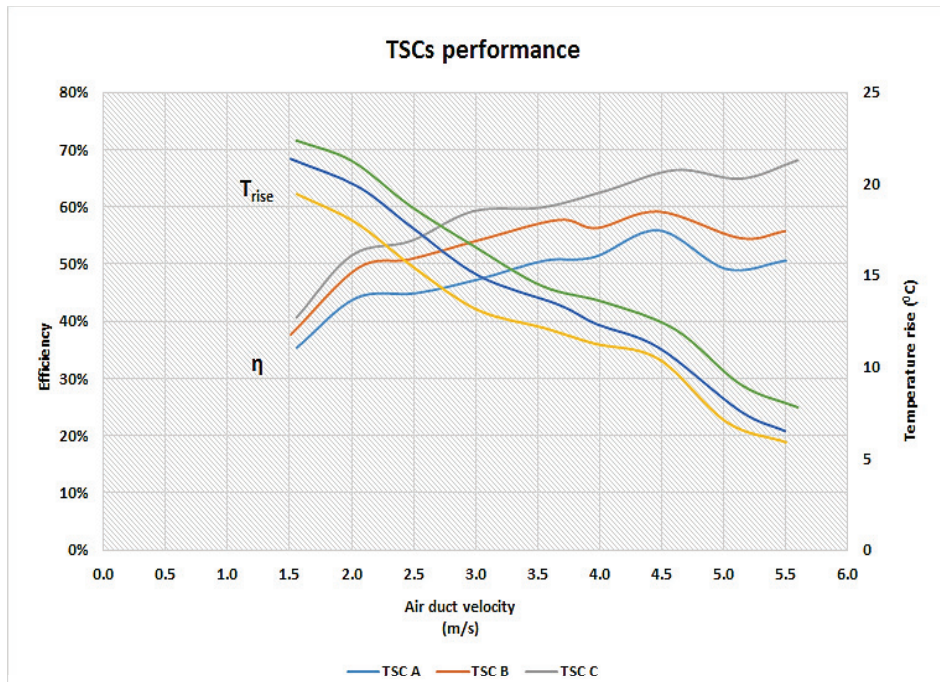


Fig. 2. Air duct velocity against efficiency and temperature rise

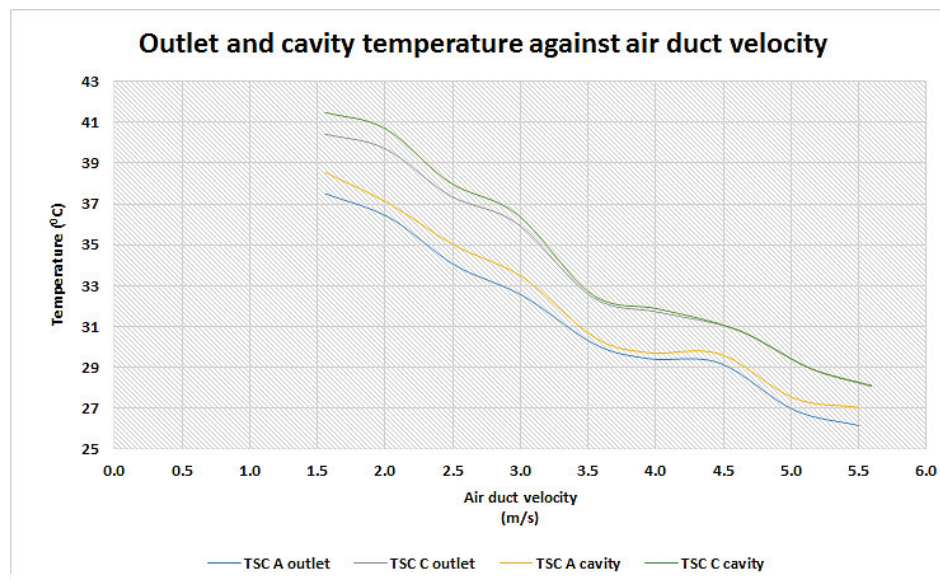


Fig. 3. Air duct velocity against outlet and cavity temperature

The thermocouple array inside each TSC was used to produce a map of temperature variation inside the cavity (figure 4, 5). Unsurprisingly, the warmest temperatures tend towards the top of the cavities. The mapping indicated clearly that below a certain flow rate ($90\text{m}^3/\text{h}$ or 3m/s), temperature variation was measurably graduated, again, with higher temperature towards the top edge. Above that flow rate the temperature inside the cavity became reasonably uniform and remained so with decreasing temperature rises and increasing air flow rates. The mapping also indicated an asymmetrical nature to the distribution at these lower flow rates, which was suspected to be linked to the wind direction.

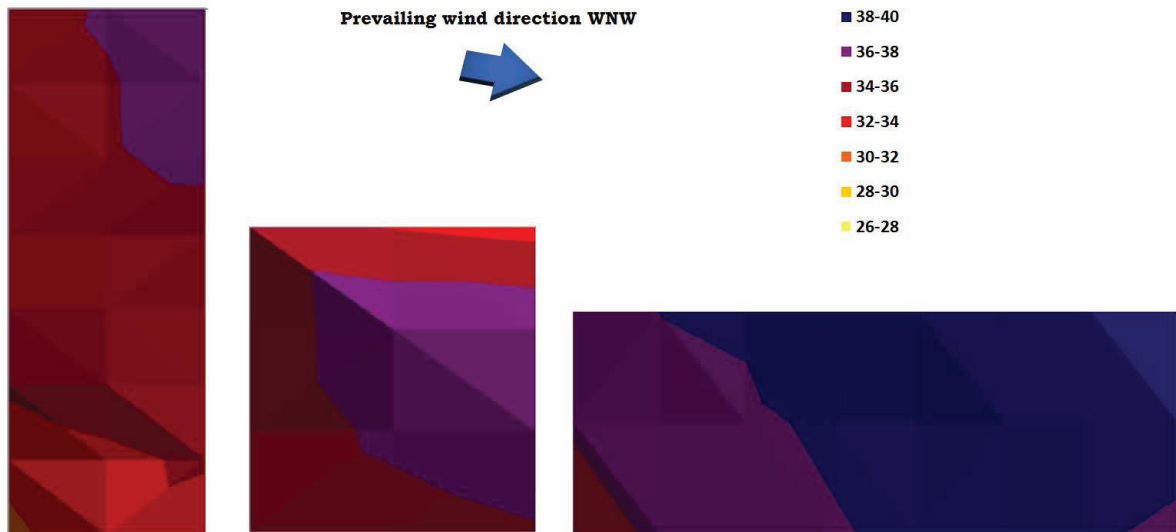


Fig. 4. Cavity temperature mapping for 2.5m/s air duct velocity

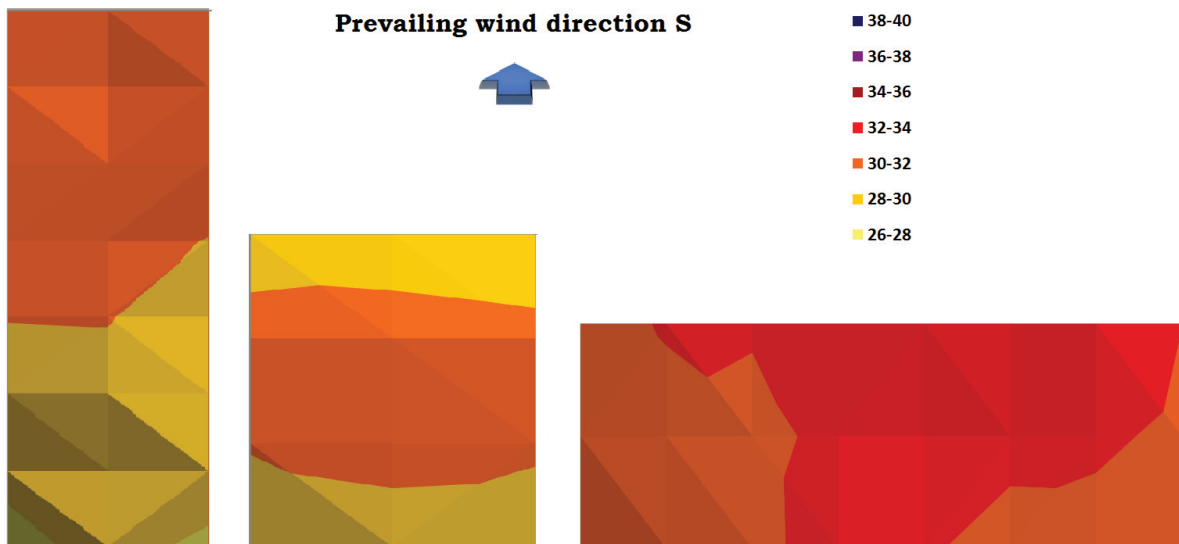


Fig. 5. Cavity temperature mapping for 4 m/s air duct velocity

Temperature sensor selection was a crucial issue as high accuracy was needed especially for low temperature rises. This study suggests that calibrated class A Pt100 sensors are appropriate for measuring the temperature in the system however when fast time response is needed calibrated type T thermocouples are also a fair choice. The thicker the sensor is the greater time response and the greater annoyance it creates to the flow inside duct. Also, wireless temperature sensors are more convenient for measuring room temperature and they should be carefully shielded or/and placed away from other heating or cooling sources.

Mass flow rate is discussed in the instrumentation section as literature underlines that this is a source of error and uncertainty. Every ducting system has its own characteristics in terms of friction, turbulence and cross sectional velocity profile. In addition the flow patterns change with different fan speeds. This study proposes a pre-testing procedure in order to determine one or more representative points for different fan speeds.

In order to estimate the uncertainty (U_η) of the efficiency equation (1) as a percentage of the efficiency result, the relative uncertainties ($U_{\dot{m}}$, U_{C_p} , $U_{T_{rise}}$, U_I , U_{A_p}) of the components of the equation have to be combined:

$$\eta \pm U_\eta = \frac{(\dot{m} \pm U_{\dot{m}})(C_p \pm U_{C_p})(T_{rise} \pm U_{T_{rise}})}{(1 \pm U_I)(A_p \pm U_{A_p})} \quad (5)$$

Each relative uncertainty was studied separately as a result of a potential random and systematic error. For an air velocity range from 1.5m/s to 5.5m/s the efficiency changed from 0.35 to 0.7 and the combined uncertainty was calculated at $\pm 15\%$ of the result. There were many difficulties related to outdoor tests in order to estimate the uncertainty with high confidence. The irradiation and wind instabilities, the cross sectional air velocity differences and the pyranometer's relatively low accuracy were the major factors in the uncertainty budget.

At the time of the development of the test rig, ISO 9806[25] had not been published, although certain elements of the approach complimented ISO 9806, such as collector position, orientation and the installation of pyranometers, it was thought that some aspects of the monitoring plan could have been improved using elements of ISO 9806. In particular, the inclusion of a pyrgeometer to measure long wave irradiance would have provided interesting data on the make-up of energy received by the collector.

However, it should be stressed that the overall purpose of the test rigs was to formulate a monitoring strategy for measuring the performance of 'in-use' TSC's, which presents a different challenge to that addressed by ISO 9806. Other than that, this aspect of the project was subject to the usual constraints of budget and resources, limiting the range and quality of instrumentation.

6. Conclusion

This paper has summarized part of the experimental research undertaken throughout the SBED project. Outdoor experimental TSCs achieved high instantaneous efficiencies (70%), however, they are subject to variable weather conditions. The shape of the collector is not the dominant performance factor, however, collectors could suffer because of parallel winds which disturb the heated air layer. Also, the position of the outlet on the back of the collectors seems to have an impact especially for low mass flows as it determines the suction forces inside the cavity. Further investigation is needed in order to quantify the effect of both wind and outlet position in real life installations. Furthermore, as TSCs become better known, a robust monitoring guideline for integrated TSC would help the market to standardise the evaluation of the real life TSC performance.

Acknowledgements

The authors gratefully acknowledge that this research was funded by the European Regional Development Fund through the Welsh Government. Also, they would like to thank Dr Vicki Stevenson and Dr Hasan Alfarra for their prior work on the TSC roof kit and Huw Jenkins and the rest of the SBED team for their valuable assistance and support.

References

1. Brown, C., et al., *Transpired Solar Collector Installations in Wales and England*. Energy Procedia, 2014. **48**(0): p. 18-27.
2. SBED. *Sustainable Building Envelope Demonstration*. 2013 22/09/2014; Available from: <http://sbed.cardiff.ac.uk/>.
3. Klein, S. and F. Alvarado, *Engineering equation solver*. F-Chart Software, Madison, WI, 2002.
4. CIBSE, *GUIDE C*, in *Reference Data*2001, Butterworth-Heinemann: Oxford.
5. Fleck, B.A., R.M. Meier, and M.D. Matovic, *A field study of the wind effects on the performance of an Unglazed Transpired Solar Collector*. Solar Energy, 2001. **73**(3): p. 8.
6. Kutscher, C., C. Christensen, and G. Barker. *Unglazed transpired solar collectors: an analytic model and test results*. in *Proceedings of ISES Solar World Congress*. 1991.
7. Kutscher, C.F., C.B. Christensen, and G.M. Barker, *Unglazed transpired solar collectors: heat loss theory*. Journal of Solar Energy Engineering, 1993. **115**(3): p. 182-188.
8. Kutscher, C., *Heat exchange effectiveness and pressure drop for air flow through perforated plates with and without crosswind*. Journal of Heat Transfer, 1994. **116**(2): p. 391-399.
9. Badache, M., S. Hallé, and D. Rousse, *A full 3 to the power of 4 factorial experimental design for efficiency optimization of an unglazed transpired solar collector prototype*. Solar Energy, 2012. **86**(9): p. 2802-2810.
10. Deans, J. and A. Weerakoon. *The thermal performance of a solar air heater*. 2008. 5th European Thermal-Sciences Conference, The Netherlands.
11. Deans, J., et al. *Use of perforated roofing sheets as solar collectors*. in *International Heat Transfer Conference 13*. 2006. Begel House Inc.
12. Weerakoon, A., et al. *Use of perforated metal sheets as solar collectors for building space heating*. in *International Heat transfer Conference*. 2004.
13. Harrison, S.J., et al., *The Characterization and Testing of Solar Collector Thermal Performance*, in *A Report of TASK III: Performance Testing of Solar Collectors*1993, International Energy Agency.
14. BS ISO, *Velocity area method using Pitot static tubes*, in *Measurements of fluid flow in closed conduits*2008, International Standards Organisation: Genova.
15. Acromag Incorporated, *A comparison of Thermocouple and RTD Temperature Sensors, Part 3*, in *Criteria for temperature sensor selection of T/C and RTD sensor types* 2011.
16. National Instruments, *How to choose the right sensor for your measurement system*, 2012.
17. Hengesbach Prozessmesstechnik, *Inserts for resistance thermometers*, 2013.
18. Nanmac Corporation, *Comparison of Temperature Sensor and Response Times*, in *White paper*2012.
19. Wilson, J.S., *Sensor technology handbook*2004: Elsevier.
20. European Association of National Metrology Institutes, *Guidelines on the Calibration of Temperature Indicators and Simulators by Electrical Simulation and Measurement*, 2011, EURAMET e.V. Technical Committee for Thermometry: Braunschweig Germany.
21. Iqbal, M., *An introduction to solar radiation*1983: Elsevier.
22. Paulescu, M., et al., *Weather modeling and forecasting of PV systems operation*2013: Springer.
23. European Association of National Metrology Institutes, *Calibration of Climatic Chambers Guidance for Calibration Laboratories*, 2011, EURAMET e.V. Technical Committee for Thermometry: Braunschweig Germany.
24. EN, B., *60584-1: 1996, IEC 60584-1: 1995*. Thermocouples. Reference tables.
25. BS ISO, *Solar energy - Solar thermal collectors - Test methods*, 2013, BSI Standards Limited 2013.